**Structural Engineering and Mechanics**, *Vol. 75, No. 6 (2020) 659-674*
DOI: https://doi.org/10.12989/sem.2020.75.6.659


# On scale–dependent stability analysis of functionally graded magneto-electro-thermo-elastic cylindrical nanoshells

Reza Asrari[1], Farzad Ebrahimi*[2] and Mohammad Mahdi Kheirikhah[1]

[1]*Faculty of Industrial and Mechanical Engineering, Qazvin Branch, Islamic Azad University, Qazvin, Iran*
[2]*Department of Mechanical Engineering, Faculty of Engineering, Imam Khomeini International University, Qazvin, Iran*

*(Received October 31, 2019, Revised March 23, 2020, Accepted April 3, 2020)*

**Abstract.** The present paper employs nonlocal strain gradient theory (NSGT) to study buckling behavior of functionally graded magneto-electro-thermo-elastic (FG-METE) nanoshells under various physical fields. NSGT modeling of the nanoshell contains two size parameters, one related to nonlocal stress field and another related to strain gradients. It is considered that mechanical, thermal, electrical and magnetic loads are exerted to the nanoshell. Temperature field has uniform and linear variation in nanoshell thickness. According to a power-law function, piezo-magnetic, thermal and mechanical properties of the nanoshell are considered to be graded in thickness direction. Five coupled governing equations have been obtained by using Hamilton's principle and then solved implementing Galerkin's method. Influences of temperature field, electric voltage, magnetic potential, nonlocality, strain gradient parameter and FG material exponent on buckling loads of the FG-METE nanoshell have been studied in detail.

**Keywords:** buckling; classical shell theory; functionally graded material; magneto-electro-thermo-elastic material; nonlocal strain gradient theory

## 1. Introduction

Magneto-electro-thermo-elastic (METE) materials as a type of intelligent materials exhibit interesting multi-physical behaviors owing to their mechanical performance under electric and magnetic fields (Pan 2001). Sensors, actuators and many smart systems and devices are good candidates for application of METE materials in them. These materials can provide electric voltage sensing or magnetic potential sensing when they are under an external mechanical load (Ebrahimi and Barati 2018). In contrast, these material can exhibit mechanical deformation when they are under electro-magnetic field (Ramirez *et al*. 2006). To achieve a METE material with expected material properties, two constituents are directly combined with each other to make a composite material such as $BaTiO_3$-$CoFe_2O_4$. The material properties of these composites including elastic moduli, piezoelectric and magnetic properties are dependent on the percentage of the two constituents. Also, $BaTiO_3$ and $CoFe_2O_4$ may be combined with each other to make a special type of material called functionally graded material (FG) (Ebrahimi and Barati 2016, Chikh *et al*. 2016, Yazid *et al*. 2018, Park *et al*. 2016, Sayyad and Ghugal 2018). In FG model, all properties are varying in thickness direction of the material. Actually, the properties can be variable form $BaTiO_3$ to $CoFe_2O_4$ or vice versa. The rate of variation in material properties is controllable in FG materials by defining a power-law model (Barati and Zenkour 2018). This model possesses a material index that makes us able to control the rate of variation.

For mathematical modeling of a nano-dimension structure such as a plate or a shell, there are different non-classic theories, for example nonlocal theory and strain gradient based theories (Eltaher *et al*. 2016, Barretta *et al*. 2016, Heydarpour and Malekzadeh 2019, Attia and Mahmoud 2016, Alasadi *et al*. 2019, Fenjan *et al*. 2019a,b, Faleh *et al*. 2020, Al-Maliki *et al*. 2019). In various models of strain gradient theory, one or more scale parameter exist in order to characterize size-dependent properties of nano-dimension structure. It is reported that structural stiffness may be increases by applying the effect of strain gradient parameter. Also, there is nonlocal theory introduced by Eringen (1983) for which it is reported that structural stiffness of nanoshells may be reduced by applying the effect of nonlocal parameter (Zeighampour *et al*. 2018). Accounting for nonlocal influences, smart nanostructures such as magneto-electro-elastic nanostructures have been studied in the view of their static or dynamic characteristics (Ke and Wang 2014, Farajpour *et al*. 2016, Ke *et al*. 2014, Waksmanski and Pan 2017, Hamad *et al*. 2019, Khalaf *et al*. 2019, Kunbar *et al*. 2020, Fenjan *et al*. 2020, Ahmed *et al*. 2020).

Many molecular dynamic simulations confirm that mechanical properties of nano-size structures rely on two scale parameters, one based on nonlocal elasticity theory and another based on strain gradient theory (Mehralian *et al*. 2017a,b). Actually, the two scale parameters must be simultaneously considered in a single theory called nonlocal strain gradient theory (NSGT). Recently, a huge number of studies have been published to explore combined nonlocal and strain gradient effects on frequencies and buckling loads of nano-size structures. NSGT is used by Ebrahimi *et*

*Corresponding author, Professor
E-mail: febrahimy@eng.ikiu.ac.ir



ISSN: 1225-4568 (Print), 1598-6217 (Online)

*al*. (2016) to examine wave dispersion characteristics of a nano-size plate constructed from FG materials. Analyzing post-buckling properties nano-size beams using NSGT has been performed by Li and Hu (2015) based on Euler-Bernoulli beam model. Employing a higher-order beam model, Lu *et al*. (2017) examined natural frequencies of a nanobeam using NSGT formulation. Analyzing nonlinear deflections and vibrational behaviors of FG nanobeams utilizing NSGT formulation have been carried out by Li and Hu (2016). Wave dispersion properties of a FG magneto-electro-elastic nano-size plate in the context of NSGT have been explored by Ebrahimi and Dabbagh (2017). Moreover, closed-form solution of deflection and natural frequency of a NAGT based FG nanobeam has been represented by Simsek (2019). Also, wave dispersion properties of a nanoshell made of FG magneto-electro-elastic material have been studied by Ma *et al*. (2018) in the framework of NSGT. Furthermore, She *et al*. (2018) examined nonlinear deflection and vibrational behaviors of NSGT-based cylindrical nanoshells with FG properties. Arefi *et al*. (2019) utilized NSGT to obtain deflections of nano-size plates having magneto-electro-elastic face sheets. Based on above information and a complete literature search, one can conclude that buckling characteristics of FG-METE nanoshells based on NSGT have not studied up to now.

Based on classical shell theory and in the context of NSGT, the present study explores buckling behavior of functionally graded magneto-electro-thermo-elastic (FG-METE) nanoshells of cylindrical shape. NSGT modeling of the nanoshell contains two size parameters, one related to nonlocal stress field and another related to strain gradients. It is considered that mechanical, thermal, electrical and magnetic loads are exerted to the nanoshell. Temperature field has uniform and linear variation in nanoshell thickness. According to a power-law function, piezo-magnetic, thermal and mechanical properties of the nanoshell are considered to be graded in thickness direction. In the context of Galerkin's method, the five governing equations are reduced to ordinary equations and are numerically solved. Impacts of thermal loading type, electric voltage, magnetic potential, nonlocal parameter, strain gradient parameter and FG material exponent on buckling loads of a FG-METE nanoshell will be figured out.

## 2. Nonlocal strain gradient shell modeling

In order to define the stress field components ($\sigma_{ij}$) in the framework of nonlocal strain gradient theory (NSGT), two stress fields which are nonlocal stress $\sigma_{ij}^{(0)}$ and higher-order stress $\sigma_{ij}^{(1)}$ have been employed (Ebrahimi *et al*. 2016):

$$\sigma_{ij} = \sigma_{ij}^{(0)} - \nabla \sigma_{ij}^{(1)} \tag{1}$$

Based on the following two integrals, nonlocal and higher-order stresses are respectively related to strain field $\varepsilon_{ij}$ and strain gradients $\nabla\varepsilon_{ij}$ with the help of nonlocal parameters ($e_0a$, $e_1a$) and strain gradient parameter ($l$) as:

$$\sigma_{ij}^{(0)} = \int_V C_{ijkl}\alpha_0(x,x',e_0a)\varepsilon'_{kl}(x')dx' \tag{2a}$$

$$\sigma_{ij}^{(1)} = l^2\int_V C_{ijkl}\alpha_1(x,x',e_1a)\nabla\varepsilon'_{kl}(x')dx' \tag{2b}$$

I above relations, $C_{ijkl}$ denotes the elastic properties. Moreover, $\alpha_0(x,x',e_0a)$ and $\alpha_1(x,x',e_1a)$ denote nonlocal Kernel functions. Differential formulation of nonlocal strain gradient theory may be represented as follows:

$$\begin{aligned}&[1-(e_1a)^2\nabla^2][1-(e_0a)^2\nabla^2]\sigma_{ij}\\&= C_{ijkl}[1-(e_1a)^2\nabla^2]\varepsilon_{kl} - C_{ijkl}\,l^2[1-(e_0a)^2\nabla^2]\nabla^2\varepsilon_{kl}\end{aligned} \tag{3}$$

The symbol $\nabla^2$ is used as Laplacian operator. By selecting $e_1 = e_0 = e$, it is possible to express a simpler formulation of NSGT as (Ebrahimi *et al*. 2016):

$$[1-(ea)^2\nabla^2]\sigma_{ij} = C_{ijkl}[1-l^2\nabla^2]\varepsilon_{kl} \tag{4}$$

## 3. FGM shell modeling

For mathematical description of a FG material, there are various models such as power-law function. Th is function may be used in order to define material properties as a function of power-law index or material gradient exponent ($p$). All of material properties ($P_f$) which may be elastic, piezoelectric and magnetic properties are variable form upper size properties ($P_t$) to bottom side properties ($P_b$) as (Faleh *et al*. 2018):

$$P_f(z) = (P_t - P_b)\left(\frac{z}{h}+\frac{1}{2}\right)^p + P_b \tag{5}$$

In above function, $z$ is distance from the mid-surface of the shell.

So far, a variety of structural theories are introduced for description and analyzes of diverse structures (Abualnour *et al*. 2019, Adda Bedia *et al*. 2019, Alimirzaei *et al*. 2019, Batou *et al*. 2019, Belbachir *et al*. 2019, Berghouti *et al*. 2019, Boukhlif *et al*. 2019, Bourada *et al*. 2019, Boutaleb *et al*. 2019, Boulefrakh *et al*. 2019, Chaabane *et al*. 2019, Draoui *et al*. 2019, Draiche *et al*. 2019, Hellal *et al*. 2019, Hussain *et al*. 2019, Karami *et al*. 2019a-c, Karami *et al*. 2020, Kaddari *et al*. 2020, Khiloun *et al*. 2019, Mahmoudi *et al*. 2019, Medani *et al*. 2019, Meksi *et al*. 2019, Sahla *et al*. 2019, Semmah *et al*. 2019, Tlidji *et al*. 2019, Zarga *et al*. 2019, Zaoui *et al*. 2019). As it is known in research community, classical shell theory (CST) is suitable for studying thin shells. However, the displacement field of the nanoshell ($u_1$, $u_2$, $u_3$) based on CST can be defined as function of axial ($u$), circumferential ($v$) and transverse ($w$) components in the following form:

$$u_1(x,y,z) = u(x,y) - z\frac{\partial w}{\partial x}(x,y) \tag{6}$$

$$u_2(x,y,z) = v(x,y) - \frac{z}{R}\frac{\partial w}{\partial y}(x,y) \tag{7}$$

$$u_3(x,y,z) = w(x,y) \tag{8}$$

There are only three strains for the CST shells as follows:

$$\begin{aligned}
\varepsilon_{xx} &= \frac{\partial u}{\partial x} - z\frac{\partial^2 w}{\partial x^2} \\
\varepsilon_{yy} &= \frac{\partial v}{\partial y} - \frac{w}{R} - z\frac{\partial^2 w}{\partial y^2} \\
\gamma_{xy} &= \frac{\partial u}{\partial y} + \frac{\partial v}{\partial x} - 2z\frac{\partial^2 w}{\partial x \partial y}
\end{aligned} \tag{9}$$

Suppose that the nanoshell is exposed to electric ($\Phi$) and magnetic ($\Upsilon$) potentials having cosine variation of electric and magnetic displacement components ($\phi$,$\gamma$) based on following relations:

$$\Phi(x,y,z) = -\cos(\xi z)\phi(x,y) + \frac{2z}{h}V \tag{10}$$

$$\Upsilon(x,y,z) = -\cos(\xi z)\gamma(x,y) + \frac{2z}{h}\Omega \tag{11}$$

It should be pointed out that $\xi=\pi/h$. Also, $V$ and $\Omega$ respectively denote exerted electric voltage and magnetic potential to nanoshell.

The electric and magnetic fields are defined as gradients of electric potential and magnetic potential, respectively. Knowing this fact, it is possible to derive all components for electrical field ($E_x$, $E_\theta$, $E_z$) and magnetic field ($H_x$, $H_\theta$, $H_z$) in the following form:

$$E_x = -\Phi_{,x} = \cos(\xi z)\frac{\partial \phi}{\partial x}, \tag{12}$$

$$E_y = -\Phi_{,y} = \cos(\xi z)\frac{\partial \phi}{\partial y}, \tag{13}$$

$$E_z = -\Phi_{,z} = -\xi \sin(\xi z)\phi - \frac{2V}{h} \tag{14}$$

$$H_x = -\Upsilon_{,x} = \cos(\xi z)\frac{\partial \gamma}{\partial x}, \tag{15}$$

$$H_y = -\Upsilon_{,y} = \cos(\xi z)\frac{\partial \gamma}{\partial y}, \tag{16}$$

$$H_z = -\Upsilon_{,z} = -\xi \sin(\xi z)\gamma - \frac{2\Omega}{h} \tag{17}$$

The components of stress field, electric field displacement ($D_x$, $D_y$, $D_z$) and magnetic induction ($B_x$, $B_y$, $B_z$) of nano-size shells according to NSGT and classical shell theory can be defined by:

$$\begin{aligned}
&(1-(ea)^2\nabla^2)\sigma_{xx} \\
&= (1-l^2\nabla^2)[\tilde{C}_{11}\varepsilon_{xx} + \tilde{C}_{12}\varepsilon_{yy}] - \tilde{e}_{31}E_z - \tilde{q}_{31}H_z - \tilde{C}_{11}\tilde{\alpha}_1\Delta T
\end{aligned} \tag{18}$$

$$\begin{aligned}
&(1-(ea)^2\nabla^2)\sigma_{yy} \\
&= (1-l^2\nabla^2)[\tilde{C}_{12}\varepsilon_{xx} + \tilde{C}_{11}\varepsilon_{yy}] - \tilde{e}_{31}E_z - \tilde{q}_{31}H_z - \tilde{C}_{11}\tilde{\alpha}_1\Delta T
\end{aligned} \tag{19}$$

$$(1-(ea)^2\nabla^2)\sigma_{x\theta} = (1-l^2\nabla^2)\tilde{C}_{66}\gamma_{x\theta} \tag{20}$$

$$(1-(ea)^2\nabla^2)D_x = +\tilde{s}_{11}E_x + \tilde{d}_{11}H_x \tag{21}$$

$$(1-(ea)^2\nabla^2)D_y = +\tilde{s}_{11}E_\theta + \tilde{d}_{11}H_\theta \tag{22}$$

$$\begin{aligned}
&(1-(ea)^2\nabla^2)D_z \\
&= (1-l^2\nabla^2)[\tilde{e}_{31}\varepsilon_{xx} + \tilde{e}_{31}\varepsilon_{yy}] + \tilde{s}_{33}E_z + \tilde{d}_{33}H_z
\end{aligned} \tag{23}$$

$$(1-(ea)^2\nabla^2)B_x = +\tilde{d}_{11}E_x + \tilde{\chi}_{11}H_x \tag{24}$$

$$(1-(ea)^2\nabla^2)B_y = +\tilde{d}_{11}E_\theta + \tilde{\chi}_{11}H_\theta \tag{25}$$

$$\begin{aligned}
&(1-(ea)^2\nabla^2)B_z \\
&= (1-l^2\nabla^2)[\tilde{q}_{31}\varepsilon_{xx} + \tilde{q}_{31}\varepsilon_{yy}] + \tilde{d}_{33}E_z + \tilde{\chi}_{33}H_z
\end{aligned} \tag{26}$$

where $\tilde{\alpha}_1$ is thermal expansion coefficient. Elastic, piezoelectric and magnetic material properties are respectively denoted by $C_{ij}$, $e_{ij}$ and $q_{ij}$. It must be mentioned that the material properties are defined in the following forms based on plane stress assumption of shells (Ke *et al*. 2014):

$$\begin{aligned}
&\tilde{C}_{11} = C_{11} - \frac{C_{13}^2}{C_{33}},\ \tilde{C}_{12} = C_{12} - \frac{C_{13}^2}{C_{33}},\ \tilde{C}_{66} = C_{66}, \\
&\tilde{e}_{31} = e_{31} - \frac{C_{13}e_{33}}{c_{33}},\quad \tilde{q}_{31} = q_{31} - \frac{C_{13}q_{33}}{C_{33}}, \\
&\tilde{d}_{11} = \tilde{d}_{11},\quad \tilde{d}_{33} = \tilde{d}_{33} + \frac{q_{33}e_{33}}{C_{33}}, \\
&\tilde{s}_{11} = s_{11},\quad \tilde{s}_{33} = s_{33} + \frac{e_{33}^2}{C_{33}},\quad \tilde{\chi}_{11} = \chi_{11}, \\
&\tilde{\chi}_{33} = \chi_{33} + \frac{q_{33}^2}{C_{33}}, \tilde{\alpha}_1 = \alpha_1 - \frac{c_{13}\alpha_3}{c_{33}}
\end{aligned} \tag{27}$$

According to the definition of strain energy ($U$) and the work done by external loads ($W$), Hamilton's principle might be expressed by:

$$\int_0^t \delta(U-W)\,dt = 0 \tag{28}$$

where

$$\begin{aligned}\delta U = \int_V & (\sigma_{xx}\delta\varepsilon_{xx} + \sigma_{xx}^{(1)}\delta\nabla\varepsilon_{xx} + \sigma_{yy}\delta\varepsilon_{yy} \\ & + \sigma_{yy}^{(1)}\delta\nabla\varepsilon_{yy} + \sigma_{xy}\delta\gamma_{xy} + \sigma_{xy}^{(1)}\delta\nabla\gamma_{xy} \\ & - D_x\delta E_x - D_y\delta E_y - D_z\delta E_z - B_x\delta H_x - B_y\delta H_y - B_z\delta H_z)\,dV\end{aligned} \tag{29}$$

$$\delta W = \int_V (N_{x0}(\frac{\partial^2 w}{\partial x^2}) + N_{y0}\frac{\partial^2 w}{\partial y^2}))\delta w\,dV \tag{30}$$

where $N_{x0}$ and $N_{\theta 0}$ are general axial and circumferential loads:

$$N_{x0} = N_{y0} = N^T + N^E + N^H + N^M \tag{31}$$

in which $N^T$, $N^E$, $N^H$, and $N^M$ respectively express temperature, electrical, magnetic and mechanical loadings. Electrical and magnetic loadings can be expressed by:

$$N^E = -\int_{-h/2}^{h/2} \tilde{e}_{31}\frac{2V}{h}dz,\ N^H = -\int_{-h/2}^{h/2} \tilde{q}_{31}\frac{2\Omega}{h}dz \tag{32}$$

Here, uniformly and linearly distributed temperature loads in the thickness of nanoshell have been considered. For the two types of temperature distribution, T(z) may be introduced by:

Uniform temperature rise:

$$T(z) = \Delta T + T_0 \tag{33}$$

Linear temperature rise:

$$T(z) = T_m + \Delta T(\frac{z}{h} + \frac{1}{2}),\ \Delta T = T_c - T_m \tag{34}$$

in which $T_c$ and $T_m$ are the temperature at top and bottom surfaces of the nanoshell thickness. Moreover, $T_0$=300 K can be defined as reference temperature. Then, temperature rise in the nanoshell can be introduced by $\Delta T$. Thermal loading through the thickness can be expressed by:

$$N^T = \int_{-h/2}^{h/2} \tilde{C}_{11}\,\tilde{\alpha}_1\,(T(z)-T_0)\,dz \tag{35}$$

By using Eq.(28) and collecting the coefficients of displacement components (δu, δv, δw), one can derive the governing equations of METE nanoshells as:

$$\frac{\partial N_{xx}}{\partial x} + \frac{\partial N_{xy}}{\partial y} = 0 \tag{36}$$

$$\frac{\partial N_{xy}}{\partial x} + \frac{\partial N_{yy}}{\partial y} = 0 \tag{37}$$

$$\begin{aligned}&\frac{\partial^2 M_{xx}}{\partial x^2} + 2\frac{\partial^2 M_{xy}}{\partial x\partial y} + \frac{\partial^2 M_{yy}}{\partial y^2} \\ &+ \frac{N_{yy}}{R} - N_{x0}(\frac{\partial^2 w}{\partial x^2}) - N_{y0}(\frac{\partial^2 w}{\partial y^2}) = 0\end{aligned} \tag{38}$$

$$\int_{-h/2}^{h/2}\left(\cos(\xi z)\frac{\partial D_x}{\partial x} + \cos(\xi z)\frac{\partial D_y}{\partial y} + \xi\sin(\xi z)D_z\right)dz = 0 \tag{39}$$

$$\int_{-h/2}^{h/2}\left(\cos(\xi z)\frac{\partial B_x}{\partial x} + \cos(\xi z)\frac{\partial B_y}{\partial y} + \xi\sin(\xi z)B_z\right)dz = 0 \tag{40}$$

where $N_{ij}$ and $M_{ij}$ (ij=xx, xy, yy) are membrane forces and bending moments:

$$\begin{aligned}N_{xx} &= \int_{-h/2}^{h/2}(\sigma_{xx}^{(0)} - \nabla\sigma_{xx}^{(1)})dz = N_{xx}^{(0)} - \nabla N_{xx}^{(1)} \\ N_{xy} &= \int_{-h/2}^{h/2}(\sigma_{xy}^{(0)} - \nabla\sigma_{xy}^{(1)})dz = N_{xy}^{(0)} - \nabla N_{xy}^{(1)} \\ N_{yy} &= \int_{-h/2}^{h/2}(\sigma_{yy}^{(0)} - \nabla\sigma_{yy}^{(1)})dz = N_{yy}^{(0)} - \nabla N_{yy}^{(1)} \\ M_{xx} &= \int_{-h/2}^{h/2} z(\sigma_{xx}^{(0)} - \nabla\sigma_{xx}^{(1)})dz = M_x^{b(0)} - \nabla M_{xx}^{b(1)} \\ M_y &= \int_{-h/2}^{h/2} z(\sigma_{yy}^{(0)} - \nabla\sigma_{yy}^{(1)})dz = M_y^{b(0)} - \nabla M_y^{b(1)} \\ M_{xy} &= \int_{-h/2}^{h/2} z(\sigma_{xy}^{(0)} - \nabla\sigma_{xy}^{(1)})dz = M_{xy}^{b(0)} - \nabla M_{xy}^{b(1)}\end{aligned} \tag{41}$$

in which

$$\begin{aligned}N_{ij}^{(0)} &= \int_{-h/2}^{h/2}(\sigma_{ij}^{(0)})dz,\quad N_{ij}^{(1)} = \int_{-h/2}^{h/2}(\sigma_{ij}^{(1)})dz \\ M_{ij}^{(0)} &= \int_{-h/2}^{h/2} z(\sigma_{ij}^{(0)})dz,\quad M_{ij}^{(1)} = \int_{-h/2}^{h/2} z(\sigma_{ij}^{(1)})dz\end{aligned} \tag{42}$$

Consider that symbols $^{(0)}$ and $^{(1)}$ respectively denote classic and non-classic forces/moments. Also, obtained boundary conditions based on Hamilton's principle can be expressed by:

$$u = 0,\ or\quad N_{xx}n_x + N_{xy}n_y = 0 \tag{43}$$

$$v = 0,\ or\quad N_{xy}n_x + N_{yy}n_y = 0 \tag{44}$$

$$\begin{aligned}&w = 0,\ or \\ &n_x(\frac{\partial M_{xx}}{\partial x} + \frac{\partial M_{xy}}{\partial y} - N_{x0}\frac{\partial w}{\partial x}) + n_y(\frac{\partial M_{yy}}{\partial y} + \frac{\partial M_{xy}}{\partial x} - N_{y0}\frac{\partial w}{\partial y}) = 0\end{aligned} \tag{45}$$

$$\frac{\partial w}{\partial x} = 0,\ or\quad M_{xx}n_x + M_{xy}n_y = 0 \tag{46}$$

$$\frac{\partial w}{\partial y} = 0,\ or\quad M_{xy}n_x + M_{yy}n_y = 0 \tag{47}$$

$$\phi = 0,\quad or\ \int_{-h/2}^{h/2}\left(\cos(\xi z)D_x n_x + \cos(\xi z)D_y n_y\right)dz = 0 \tag{48}$$

$$\gamma = 0,\quad or\ \int_{-h/2}^{h/2}\left(\cos(\xi z)B_x n_x + \cos(\xi z)B_y n_y\right)dz = 0 \tag{49}$$

in which $n_x$ and $n_y$ denote cosines of direction.

By integrating Eq. (41) over the thickness, one may derive following relations based on NSGT formulation of METE nanoshells:

$$(1-(ea)^2\nabla^2)N_{xx}=(1-l^2\nabla^2)[A_{11}\frac{\partial u}{\partial x}-B_{11}\frac{\partial^2 w}{\partial x^2}+A_{12}(\frac{\partial v}{\partial y}-\frac{w}{R})-B_{12}\frac{\partial^2 w}{\partial y^2})] \\ +A_{31}^e\phi+A_{31}^m\gamma-N^T-N^E-N^H \tag{50}$$

$$(1-(ea)^2\nabla^2)M_{xx}=(1-l^2\nabla^2)[B_{11}\frac{\partial u}{\partial x}-D_{11}\frac{\partial^2 w}{\partial x^2}+B_{12}(\frac{\partial v}{\partial y}-\frac{w}{R})-D_{12}\frac{\partial^2 w}{\partial y^2}] \\ +E_{31}^e\phi+E_{31}^m\gamma \tag{51}$$

$$(1-(ea)^2\nabla^2)N_{\theta\theta}=(1-l^2\nabla^2)[A_{12}\frac{\partial u}{\partial x}-B_{12}\frac{\partial^2 w}{\partial x^2}+A_{11}(\frac{\partial v}{\partial y}-\frac{w}{R})-B_{11}\frac{\partial^2 w}{\partial y^2}] \\ +A_{31}^e\phi+A_{31}^m\gamma \tag{52}$$

$$(1-(ea)^2\nabla^2)M_{\theta\theta}=(1-l^2\nabla^2)[B_{12}\frac{\partial u}{\partial x}-D_{12}\frac{\partial^2 w}{\partial x^2}+B_{11}(\frac{\partial v}{\partial y}-\frac{w}{R})-D_{11}\frac{\partial^2 w}{\partial y^2}] \\ +E_{31}^e\phi+E_{31}^m\gamma \tag{53}$$

$$(1-(ea)^2\nabla^2)N_{x\theta}=(1-l^2\nabla^2)[A_{66}(\frac{\partial u}{\partial y}+\frac{\partial v}{\partial x})-2B_{66}\frac{\partial^2 w}{\partial x\partial y}] \tag{54}$$

$$(1-(ea)^2\nabla^2)M_{x\theta}=(1-l^2\nabla^2)[B_{66}(\frac{\partial u}{\partial y}+\frac{\partial v}{\partial x})-2D_{66}\frac{\partial^2 w}{\partial x\partial y}] \tag{55}$$

$$\int_{-h/2}^{h/2}(1-(ea)^2\nabla^2)D_x\cos(\xi z)dz=+F_{11}^e\frac{\partial\phi}{\partial x}+F_{11}^m\frac{\partial\gamma}{\partial x} \tag{56}$$

$$\int_{-h/2}^{h/2}(1-(ea)^2\nabla^2)D_y\cos(\xi z)dz=+F_{22}^e\frac{\partial\phi}{\partial y}+F_{22}^m\frac{\partial\gamma}{\partial y} \tag{57}$$

$$(1-(ea)^2\nabla^2)\int_{-h/2}^{h/2}D_z\,\xi\sin(\xi z)dz=A_{31}^e(\frac{\partial u}{\partial x})+A_{31}^e(\frac{\partial v}{\partial y}-\frac{w}{R})-E_{31}^e(\frac{\partial^2 w}{\partial x^2}+\frac{\partial^2 w}{\partial y^2}) \\ -F_{33}^e\phi-F_{33}^m\gamma \tag{58}$$

$$\int_{-h/2}^{h/2}(1-(ea)^2\nabla^2)B_x\cos(\xi z)dz=+F_{11}^m\frac{\partial\phi}{\partial x}+X_{11}^m\frac{\partial\gamma}{\partial x} \tag{59}$$

$$\int_{-h/2}^{h/2}(1-(ea)^2\nabla^2)B_y\cos(\xi z)dz=+F_{22}^m\frac{\partial\phi}{\partial y}+X_{22}^m\frac{\partial\gamma}{\partial y} \tag{60}$$

$$\int_{-h/2}^{h/2}(1-(ea)^2\nabla^2)B_z\,\xi\sin(\xi z)dz=A_{31}^m(\frac{\partial u}{\partial x})+A_{31}^m(\frac{\partial v}{\partial y}-\frac{w}{R})-E_{31}^m(\frac{\partial^2 w}{\partial x^2}+\frac{\partial^2 w}{\partial y^2}) \\ -F_{33}^m\phi-X_{33}^m\gamma \tag{61}$$

in which

$$\{A_{11}, B_{11}, D_{11}\} = \int_{-h/2}^{h/2} \tilde{C}_{11} \{1, z, z^2\} dz, \tag{62}$$

$$\{A_{12}, B_{12}, D_{12}\} = \int_{-h/2}^{h/2} \tilde{C}_{12} \{1, z, z^2\} dz, \tag{63}$$

$$\{A_{66}, B_{66}, D_{66}\} = \int_{-h/2}^{h/2} \tilde{C}_{66} \{1, z, z^2\} dz, \tag{64}$$

$$\left\{A_{31}^e, E_{31}^e\right\} = \int_{-h/2}^{h/2} \tilde{e}_{31} \xi \sin(\xi z) \left\{1, z\right\} dz \tag{65}$$

$$\left\{A_{31}^m, E_{31}^m\right\} = \int_{-h/2}^{h/2} \tilde{q}_{31} \xi \sin(\xi z) \left\{1, z\right\} dz \tag{66}$$

$$\begin{aligned} &\left\{F_{11}^e, F_{22}^e, F_{33}^e\right\} \\ &= \int_{-h/2}^{h/2} \left\{\tilde{s}_{11} \cos^2(\xi z), \tilde{s}_{22} \cos^2(\xi z), \tilde{s}_{33} \xi^2 \sin^2(\xi z)\right\} dz \end{aligned} \tag{67}$$

$$\begin{aligned} &\left\{F_{11}^m, F_{22}^m, F_{33}^m\right\} \\ &= \int_{-h/2}^{h/2} \left\{\tilde{d}_{11} \cos^2(\xi z), \tilde{d}_{22} \cos^2(\xi z), \tilde{d}_{33} \xi^2 \sin^2(\xi z)\right\} dz \end{aligned} \tag{68}$$

$$\begin{aligned} &\left\{X_{11}^m, X_{22}^m, X_{33}^m\right\} \\ &= \int_{-h/2}^{h/2} \left\{\tilde{\chi}_{11} \cos^2(\xi z), \tilde{\chi}_{22} \cos^2(\xi z), \tilde{\chi}_{33} \xi^2 \sin^2(\xi z)\right\} dz \end{aligned} \tag{69}$$

The governing equations for METE in the context of NSGT can be obtained in terms of displacement variables by substituting Eqs.(50)-(61) into Eqs.(36)-(40) as:

$$\begin{aligned} &(1-l^2\nabla^2)[A_{11}\frac{\partial^2 u}{\partial x^2} - B_{11}\frac{\partial^3 w}{\partial x^3} + A_{12}(\frac{\partial^2 v}{\partial x \partial y} - \frac{1}{R}\frac{\partial w}{\partial x}) - B_{12}\frac{\partial^3 w}{\partial x \partial y^2} + A_{66}(\frac{\partial^2 u}{\partial y^2} + \frac{\partial^2 v}{\partial x \partial y}) \\ &-2B_{66}\frac{\partial^3 w}{\partial x \partial y^2}] + A_{31}^e\frac{\partial \phi}{\partial x} + A_{31}^m\frac{\partial \gamma}{\partial x} = 0 \end{aligned} \tag{70}$$

$$\begin{aligned} &(1-l^2\nabla^2)[A_{66}(\frac{\partial^2 u}{\partial x \partial y} + \frac{\partial^2 v}{\partial x^2}) - 2B_{66}\frac{\partial^3 w}{\partial x^2 \partial y} + A_{12}\frac{\partial^2 u}{\partial x \partial y} - B_{12}\frac{\partial^3 w}{\partial x^2 \partial y} + A_{11}(\frac{\partial^2 v}{\partial y^2} - \frac{1}{R}\frac{\partial w}{\partial y}) - B_{11}\frac{\partial^3 w}{\partial y^3}] \\ &+A_{31}^e\frac{\partial \phi}{\partial y} + A_{31}^m\frac{\partial \gamma}{\partial y} = 0 \end{aligned} \tag{71}$$

$$\begin{aligned} &(1-l^2\nabla^2)[B_{11}\frac{\partial^3 u}{\partial x^3} - D_{11}\frac{\partial^4 w}{\partial x^4} + B_{12}(\frac{\partial^3 v}{\partial x^2 \partial y} - \frac{1}{R}\frac{\partial^2 w}{\partial x^2}) - D_{12}\frac{\partial^4 w}{\partial x^2 \partial y^2} + 2B_{66}(\frac{\partial^3 u}{\partial x \partial y^2} + \frac{\partial^3 v}{\partial x^2 \partial y}) \\ &-4D_{66}\frac{\partial^4 w}{\partial x^2 \partial y^2} + B_{12}\frac{\partial^3 u}{\partial x \partial y^2} - D_{12}\frac{\partial^4 w}{\partial x^2 \partial y^2} + B_{11}(\frac{\partial^3 v}{\partial y^3} - \frac{1}{R}\frac{\partial^2 w}{\partial y^2}) - D_{11}\frac{\partial^4 w}{\partial y^4} \\ &+\frac{A_{12}}{R}\frac{\partial u}{\partial x} - \frac{B_{12}}{R}\frac{\partial^2 w}{\partial x^2} + \frac{A_{11}}{R}(\frac{\partial v}{\partial y} - \frac{w}{R}) - \frac{B_{11}}{R}\frac{\partial^2 w}{\partial y^2}] + E_{31}^e(\frac{\partial^2 \phi}{\partial x^2} + \frac{\partial^2 \phi}{\partial y^2}) + E_{31}^m(\frac{\partial^2 \gamma}{\partial x^2} + \frac{\partial^2 \gamma}{\partial y^2}) + \frac{A_{31}^e}{R}\phi + \frac{A_{31}^m}{R}\gamma \\ &+(1-(ea)^2\nabla^2)[-(N^T + N^E + N^H + N^M)(\frac{\partial^2 W}{\partial x^2} + \frac{\partial^2 W}{\partial y^2})] = 0 \end{aligned} \tag{72}$$

$$+F_{11}^{e}\frac{\partial^2\phi}{\partial x^2}+F_{11}^{m}\frac{\partial^2\gamma}{\partial x^2}+F_{22}^{e}\frac{\partial^2\phi}{\partial y^2}+F_{22}^{m}\frac{\partial^2\gamma}{\partial y^2}+A_{31}^{e}(\frac{\partial u}{\partial x}+\frac{\partial v}{\partial y}-\frac{w}{R})-E_{31}^{e}(\frac{\partial^2 w}{\partial x^2}+\frac{\partial^2 w}{\partial y^2}) \tag{73}$$
$$-F_{33}^{e}\phi-F_{33}^{m}\gamma=0$$

$$+F_{11}^{m}\frac{\partial^2\phi}{\partial x^2}+X_{11}^{m}\frac{\partial^2\gamma}{\partial x^2}+F_{22}^{m}\frac{\partial^2\phi}{\partial y^2}+X_{22}^{m}\frac{\partial^2\gamma}{\partial y^2}+A_{31}^{m}(\frac{\partial u}{\partial x}+\frac{\partial v}{\partial y}-\frac{w}{R})-E_{31}^{m}(\frac{\partial^2 w}{\partial x^2}+\frac{\partial^2 w}{\partial y^2}) \tag{74}$$
$$-F_{33}^{m}\phi-X_{33}^{m}\gamma=0$$

## 4. Solution procedure

Galerkin's technique is an effective method for solving five coupled governing equations of METE nanoshells. The nanoshell boundary conditions in axial direction (at $x$=0 and $L$) can be assumed as:

$$\phi=\gamma=w=\frac{\partial^2 w}{\partial x^2}=\frac{\partial^4 w}{\partial x^4}=0 \tag{75}$$

Simply-supported edges

$$\phi=\gamma=w=\frac{\partial w}{\partial x}=0 \tag{76}$$

Clamped edges

The displacement components must be accurately determined in order to verify above boundary conditions. To this end, an approximate solution for the five variables can be considered as:

$$u=\sum_{m=1}^{\infty}\sum_{n=1}^{\infty}U_{mn}\bar{u}(x,y)=\sum_{m=1}^{\infty}\sum_{n=1}^{\infty}U_{mn}\frac{\partial X_m(x)}{\partial x}Y_n(y) \tag{77}$$

$$v=\sum_{m=1}^{\infty}\sum_{n=1}^{\infty}V_{mn}\bar{v}(x,y)=\sum_{m=1}^{\infty}\sum_{n=1}^{\infty}V_{mn}X_m(x)\frac{\partial Y_n(y)}{\partial y} \tag{78}$$

$$w=\sum_{m=1}^{\infty}\sum_{n=1}^{\infty}W_{mn}\bar{w}(x,y)=\sum_{m=1}^{\infty}\sum_{n=1}^{\infty}W_{mn}X_m(x)Y_n(y) \tag{79}$$

$$\phi=\sum_{m=1}^{\infty}\sum_{n=1}^{\infty}\Phi_{mn}\bar{\phi}(x,y)=\sum_{m=1}^{\infty}\sum_{n=1}^{\infty}\Phi_{mn}X_m(x)Y_n(y) \tag{80}$$

$$\gamma=\sum_{m=1}^{\infty}\sum_{n=1}^{\infty}\Upsilon_{mn}\bar{\gamma}(x,y)=\sum_{m=1}^{\infty}\sum_{n=1}^{\infty}\Upsilon_{mn}X_m(x)Y_n(y) \tag{81}$$

where $U_{mn}$, $V_{mn}$, $W_{mn}$, $\Phi_{mn}$ and $\Upsilon_{mn}$ are buckling amplitudes. Two functions $X_m$ and $Y_n$ must be selected in suitable forms for capturing the influences of boundary conditions:

Both edges simply-supported (S-S):

$$X_m=\sin(\frac{m\pi}{L}x),\ Y_n=\sin(ny) \tag{82}$$

Both edges clamped (C-C):

$$X_m=\sin^2(\frac{m\pi}{L}x),\ Y_n=\mathrm{Sin}(ny) \tag{83}$$

Based on Galerkin's technique and inserting displacement components in Eqs.(77)-(81) to Eqs.(70)-(74), the governing equations can be presented as ordinary equations:

$$k_{11}U+k_{21}V+k_{31}W+k_{41}\Phi+k_{51}\Upsilon=0 \tag{84}$$

$$k_{12}U+k_{22}V+k_{32}W+k_{42}\Phi+k_{52}\Upsilon=0 \tag{85}$$

$$k_{13}U+k_{23}V+k_{33}W+k_{43}\Phi+k_{53}\Upsilon=0 \tag{86}$$

$$k_{14}U+k_{24}V+k_{34}W+k_{44}\Phi+k_{54}\Upsilon=0 \tag{87}$$

$$k_{15}U+k_{25}V+k_{35}W+k_{45}\Phi+k_{55}\Upsilon=0 \tag{88}$$

Representing above equations in matrix form gives:

$$[K]\begin{bmatrix}U\\V\\W\\\Phi\\\Upsilon\end{bmatrix}=0 \tag{89}$$

where [K] denotes the stiffness matrix of nanoshell; $k_{ij}$ are stiffness matrix components which have the following definitions:

$$k_{11}=\int_0^L\int_0^{2\pi R}((1-l^2\nabla^2)[A_{11}\frac{\partial^2\bar{u}}{\partial x^2}+A_{66}(\frac{\partial^2\bar{u}}{\partial y^2})])\bar{u}(x,y)dydx \tag{90}$$

$$k_{21}=\int_0^L\int_0^{2\pi R}((1-l^2\nabla^2)[A_{12}(\frac{\partial^2\bar{v}}{\partial x\partial y})+A_{66}(\frac{\partial^2\bar{v}}{\partial x\partial y})])\bar{u}(x,y)dydx \tag{91}$$

$$k_{31}=\int_0^L\int_0^{2\pi R}((1-l^2\nabla^2)[-B_{11}\frac{\partial^3 w}{\partial x^3}+A_{12}(-\frac{1}{R}\frac{\partial w}{\partial x})-B_{12}\frac{\partial^3 w}{\partial x\partial y^2}-2B_{66}\frac{\partial^3 w}{\partial x\partial y^2}]])u(x,y)dydx \tag{92}$$

$$k_{41}=\int_0^L\int_0^{2\pi R}(A_{31}^e\frac{\partial \phi}{\partial x})u(x,y)dydx \tag{93}$$

$$k_{51}=\int_0^L\int_0^{2\pi R}(A_{31}^m\frac{\partial \gamma}{\partial x})u(x,y)dydx \tag{94}$$

$$k_{12}=\int_0^L\int_0^{2\pi R}((1-l^2\nabla^2)[A_{66}(\frac{\partial^2 u}{\partial x\partial y})+A_{12}\frac{\partial^2 u}{\partial x\partial y}])v(x,y)dydx \tag{95}$$

$$k_{22}=\int_0^L\int_0^{2\pi R}((1-l^2\nabla^2)[A_{66}(\frac{\partial^2 v}{\partial x^2})+A_{11}(\frac{\partial^2 v}{\partial y^2})])v(x,y)dydx \tag{96}$$

$$k_{32}=\int_0^L\int_0^{2\pi R}((1-l^2\nabla^2)[-2B_{66}\frac{\partial^3 w}{\partial x^2\partial y}-B_{12}\frac{\partial^3 w}{\partial x^2\partial y}+A_{11}(-\frac{1}{R}\frac{\partial w}{\partial y})-B_{11}\frac{\partial^3 w}{\partial y^3}])v(x,y)dydx \tag{97}$$

$$k_{42}=\int_0^L\int_0^{2\pi R}(+A_{31}^e\frac{\partial \phi}{\partial y})v(x,y)dydx \tag{98}$$

$$k_{52}=\int_0^L\int_0^{2\pi R}(+A_{31}^m\frac{\partial \gamma}{\partial y})v(x,y)dydx \tag{99}$$

$$k_{13}=\int_0^L\int_0^{2\pi R}((1-l^2\nabla^2)[B_{11}\frac{\partial^3 u}{\partial x^3}+2B_{66}(\frac{\partial^3 u}{\partial x\partial y^2})+B_{12}\frac{\partial^3 u}{\partial x\partial y^2}+\frac{A_{12}}{R}\frac{\partial u}{\partial x}])w(x,y)dydx \tag{100}$$

$$k_{23}=\int_0^L\int_0^{2\pi R}((1-l^2\nabla^2)[+B_{12}(\frac{\partial^3 v}{\partial x^2\partial y})+2B_{66}(\frac{\partial^3 v}{\partial x^2\partial y})+B_{11}(\frac{\partial^3 v}{\partial y^3})+\frac{A_{11}}{R}(\frac{\partial v}{\partial y})])w(x,y)dydx \tag{101}$$

$$\begin{aligned}k_{33}=&\int_0^L\int_0^{2\pi R}((1-l^2\nabla^2)[-D_{11}\frac{\partial^4 w}{\partial x^4}+B_{12}(-\frac{1}{R}\frac{\partial^2 w}{\partial x^2})-2D_{12}\frac{\partial^4 w}{\partial x^2\partial y^2}-4D_{66}\frac{\partial^4 w}{\partial x^2\partial y^2}\\&+B_{11}(-\frac{1}{R}\frac{\partial^2 w}{\partial y^2})-D_{11}\frac{\partial^4 w}{\partial y^4}-\frac{B_{12}}{R}\frac{\partial^2 w}{\partial x^2}+\frac{A_{11}}{R}(-\frac{w}{R})-\frac{B_{11}}{R}\frac{\partial^2 w}{\partial y^2}]\\&+(1-(ea)^2\nabla^2)[-(N^T+N^E+N^H+N^M)(\frac{\partial^2 w}{\partial x^2}+\frac{\partial^2 w}{\partial y^2})])w(x,y)dydx\end{aligned} \tag{102}$$

$$k_{43}=\int_0^L\int_0^{2\pi R}(+E_{31}^e(\frac{\partial^2 \phi}{\partial x^2}+\frac{\partial^2 \phi}{\partial y^2})+\frac{A_{31}^e}{R}\phi)w(x,y)dydx \tag{103}$$

$$k_{53}=\int_0^L\int_0^{2\pi R}(+E_{31}^m(\frac{\partial^2\gamma}{\partial x^2}+\frac{\partial^2\gamma}{\partial y^2})+\frac{A_{31}^m}{R}\gamma)w(x,y)dydx \quad (104)$$

$$k_{14}=\int_0^L\int_0^{2\pi R}(+A_{31}^e(\frac{\partial u}{\partial x}))\phi(x,y)dydx \quad (105)$$

$$k_{24}=\int_0^L\int_0^{2\pi R}(+A_{31}^e(+\frac{\partial v}{\partial y}))\phi(x,y)dydx \quad (106)$$

$$k_{34}=\int_0^L\int_0^{2\pi R}(+A_{31}^e(-\frac{w}{R})-E_{31}^e(\frac{\partial^2 w}{\partial x^2}+\frac{\partial^2 w}{\partial y^2}))\phi(x,y)dydx \quad (107)$$

$$k_{44}=\int_0^L\int_0^{2\pi R}(+F_{11}^e\frac{\partial^2\phi}{\partial x^2}+F_{22}^e\frac{\partial^2\phi}{\partial y^2}-F_{33}^e\phi)\phi(x,y)dydx \quad (108)$$

$$k_{54}=\int_0^L\int_0^{2\pi R}(+F_{11}^m\frac{\partial^2\gamma}{\partial x^2}+F_{22}^m\frac{\partial^2\gamma}{\partial y^2}-F_{33}^m\gamma)\phi(x,y)dydx \quad (109)$$

$$k_{15}=\int_0^L\int_0^{2\pi R}(+A_{31}^m(\frac{\partial u}{\partial x}))\gamma(x,y)dydx \quad (110)$$

$$k_{25}=\int_0^L\int_0^{2\pi R}(+A_{31}^m(+\frac{\partial v}{\partial y}))\gamma(x,y)dydx \quad (111)$$

$$k_{35}=\int_0^L\int_0^{2\pi R}(+A_{31}^m(-\frac{w}{R})-E_{31}^m(\frac{\partial^2 w}{\partial x^2}+\frac{\partial^2 w}{\partial y^2}))\gamma(x,y)dydx \quad (112)$$

$$k_{55}=\int_0^L\int_0^{2\pi R}(+X_{11}^m\frac{\partial^2\overline{\gamma}}{\partial x^2}+X_{22}^m\frac{\partial^2\overline{\gamma}}{\partial y^2}-X_{33}^m\overline{\gamma})\overline{\gamma}(x,y)dydx \quad (113)$$

In order to find the values of buckling load, the determinant of stiffness matrix should be defined as zero. Nonlocal parameter, strain gradient parameter and buckling load have been normalized as:

$$\overline{N}=N^M\frac{L}{c_{11}^t h},\ \mu=\frac{ea}{L},\ \lambda=\frac{l}{L} \quad (114)$$

## 5. Numerical results and discussions

Thorough this section, buckling characteristics of FG-METE nanoshells under thermal loading, electric voltages, magnetic potentials and mechanical loading have been studied in detail. Influences of NSGT scale coefficients and material exponent of FG material on buckling loads have been investigated. Geometry of the METE nanoshell has been illustrated in Fig.1. Table 1 presents the material properties of FG-METE material.

For validating buckling loads of a FG cylindrical shell, obtained buckling loads are compared with the results provided by Bitch *et al*. (2013) in Table 2 for two buckling modes of (m,n)=(1,3) and (1,5). Different values of material exponent (p=0, 0.5, 1, 5) are considered for this comparison. Also, nonlocal and strain gradient effects have been discarded. Obtained buckling loads are the same as those reported by Bitch *et al*. (2013). Taking into account nonlocal strain gradient influences, the buckling loads of cylindrical nanoshells are validated in Table 3 with those of Mehralian *et al*. (2017) using molecular dynamic (MD) simulation. A nanoshell of radius R=2nm has been considered for this comparison. Based on calibrated values of nonlocal and strain gradient parameters, obtained results in present show good agreement with those of Mehralian *et al*. (2017).

In the view of structural analysis, a compressive load can decrease structural stiffness of a shell. When the compressive load is strong enough, it can lead to buckling of the shells. In the same way, exerting a high temperature can lead to structural stiffness reduction and then thermal buckling of the shells at critical buckling temperature. Tables 4 and 5 represent critical buckling loads and buckling temperatures of FG-METE cylindrical nanoshells with S-S edge conditions for different material gradient exponents ($p$), nonlocal parameters (μ) and strain gradient parameters (λ). By choosing μ=λ=0, buckling loads and buckling temperatures of macro-scale shells can be derived.

Hence, non-zero values for nonlocal and strain gradient parameters may reflect scale-dependent effects. In the case of λ=0, small scale effects are considered using nonlocal elasticity theory and strain gradient effect has been ignored. It can be understand from the tables that increasing in nonlocal parameter may reduce buckling loads and temperatures of METE nanoshell. Also, strain gradient growth can give greater buckling load at fixed material gradient exponent. However, buckling behavior of FG nanoshells depends on material exponent value. Indeed, increase of $p$ leads to smaller buckling load owing to reduction in amount of $CoFe_2O_4$ with lower elastic moduli compared to $BaTiO_3$.

In Fig.2, variation of critical buckling load of METE nanoshell with respect to electric voltage ($V$) has been plotted for different values of material gradient exponent ($p$). Different elasticity theories have been considered: classical elasticity theory (CET) with μ=0, λ=0, nonlocal elasticity theory (NET) with μ=0.03, λ=0 and nonlocal strain gradient theory (NSGT) with μ=0.03, λ=0.02. In can be deduced from the figure that NSGT gives greater buckling loads than NET. This is because NSGT considers the influence of strain gradients and structural stiffness increment. NSGT is also able to consider structural stiffness reduction by using nonlocal stress field effects. However, NET only introduces structural stiffness reduction and gives smaller buckling loads than CET. An important fact is that at $p$=0, the nanoshell of 100% made of $CoFe_2O_4$ for the value of piezoelectric constant ($e_{31}$) is zero for it. Therefore,

the nanoshell buckling is not affected by the electric voltage when $p$=0. Also, as the value of $p$ rises, the total portion of $CoFe_2O_4$ in FG material reduces and then the buckling load becomes more influenced by the electric voltage. Thus, the buckling load decrease occurs with higher rate as the value of material exponent growths. For non-zero-values of material exponent, the nanoshell buckling load diminishes due to increase of applied voltage. Indeed, positive voltage may results in smaller buckling load than negative voltage.

Fig. 3 demonstrates buckling load variation of the nanoshell with respect to applied magnetic potential ($\Omega$) and material gradient exponent ($p$) based on various elasticity theories (CET, NET and NSGT). Simply-supported boundary conditions have been considered for the nanoshell. Again, it can be observed that NET modeling of the nanoshell leads to lower buckling loads compared to CET or NSGT. Also, it can be seen that the nanoshell buckling load increases due to increase of applied magnetic potential. However, positive magnetic field may results in grater buckling load than negative magnetic field. Moreover, buckling behavior of FG-METE nanoshell in magnetic field relies on the value of material exponent ($p$). As the value of p is smaller, the buckling load curves magnetic potential increases with higher rates. This is because the percentage of magnet phase ($CoFe_2O_4$) is greater than piezoelectric phase at lower material exponents.

Fig. 4 indicates critical buckling temperature of FG-METE nanoshells With S-S and C-C boundary conditions exposed to uniform temperature rise (UTR) and linear temperature rise (LTR) by varying nonlocal and strain gradient coefficients. Regardless of the type of temperature file, critical buckling temperature diminishes with the growth of nonlocal parameter, but increases with increasing in strain gradient parameter. Therefore, this two scale parameters have different effects on buckling of nanoshells. Another observation from the figure is that UTR leads to lower critical temperatures than LTR since the nanoshell is more flexible under UTR. So, the nanoshell can tolerate higher temperatures in the case of LTR.

Coupled effects of magneto-electro-thermal fields on buckling behavior of FG-METE nanoshells have been illustrated in Fig.5. To this end, buckling temperature of the nanoshell has been plotted versus magnetic potential based on different values of electric voltage. Both uniform and linear temperature rises are considered. It is evident from this figure that critical temperature generally increases by changing of magnet potential from a negative to positive value. While, critical temperature reduces by changing of electric voltage from a negative value to a positive value. Indeed, negative electric voltages represent greater buckling load than positive voltages because negative voltage induce a tensile force to the nanoshell while positive voltages induce a compressive force to the nanoshell.

Fig. 6 depicts critical buckling temperatures of FG-METE nanoshells with respect to circumferential wave number (n) and different nonlocal parameters. Temperature field has been considered to be uniform, UTR. It can be concluded from the figure that buckling temperatures first reduce with wave number and then increase with wave number. This behavior is owing to complex configuration of nanoshells at various buckling modes. Moreover, it can be observed that nonlocal parameter has its reducing effect on buckling temperature at all values of circumferential wave number.

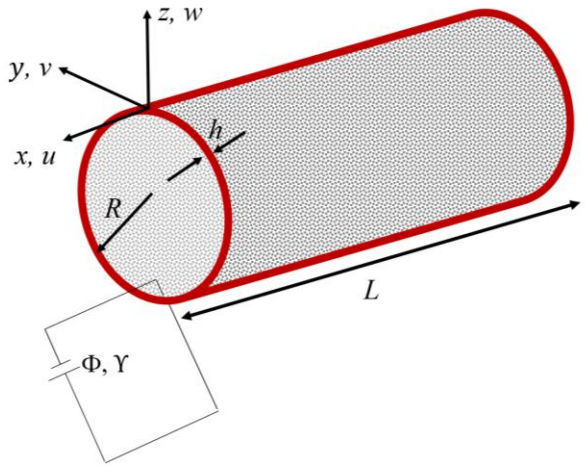


Fig. 1 Geometry of a METE cylindrical nanoshell.

Table 1 Material properties of the FG-METE nanoshell.

| Properties | $BaTiO_3$ | $CoFe_2O_4$ |
|---|---|---|
| $c_{11}=c_{22}$ (GPa) | 166 | 286 |
| $c_{12}$ | 77 | 173 |
| $c_{66}$ | 44.5 | 56.5 |
| $e_{31}$ ($Cm^{-2}$) | -4.4 | 0 |
| $q_{31}$ (N/Am) | 0 | 580.3 |
| $s_{11}$ ($10^{-9}\,C^2\,m^{-2}\,N^{-1}$) | 11.2 | 0.08 |
| $s_{33}$ | 12.6 | 0.093 |
| $\chi_{11}$($10^{-6}\,Ns^2C^{-2}/2$) | 5 | -590 |
| $\chi_{33}$ | 10 | 157 |
| $d_{11}=d_{22}=d_{33}$ | 0 | 0 |
| $\alpha_1$($10^{-6}1/K$) | 10 | 15.7 |

Table 2 Comparison of buckling load for a FG cylindrical shell (R/h=100)

| | | Bitch et al. (2013) | Present study |
|---|---|---|---|
| L/R=2 | p=0 | 2.229 | 2.229 |
| (m,n)=(1,5) | p =0.5 | 1.545 | 1.545 |
| | p =1 | 1.228 | 1.228 |
| | p=5 | 0.723 | 0.723 |
| L/R=6 | p=0 | 2.079 | 2.079 |
| (m,n)=(1,3) | p =0.5 | 1.445 | 1.445 |
| | p =1 | 1.151 | 1.150 |
| | p=5 | 0.674 | 0.674 |

Table 3 Validation of buckling loads for NSGT nanoshell (L/R=10, h/R=0.2)

| | $\lambda$=0.5 nm$^2$ | | $\lambda$=0.7 nm$^2$ | |
|---|---|---|---|---|
| | Mehralian et al. (2017) | Present | Mehralian et al. (2017) | Present |
| $\mu$=1 | 372.225 | 372.880 | 395.186 | 395.881 |
| $\mu$ =1.3 | 324.044 | 324.614 | 344.033 | 344.638 |
| $\mu$ =1.5 | 293.239 | 293.775 | 311.327 | 311.875 |

Table 4 Buckling load of FG nanoshell based on various material gradient index, nonlocal and strain gradient parameters (V=0, Ω=0, L=20R, R=50h).

| | $\lambda$=0 | $\lambda$=0.01 | $\lambda$=0.02 |
|---|---|---|---|
| p=0 $\mu$=0 | 3.26619 | 3.40006 | 3.80165 |
| $\mu$=0.01 | 3.13759 | 3.26618 | 3.65197 |
| $\mu$=0.02 | 2.80613 | 2.92114 | 3.26617 |
| $\mu$=0.03 | 2.38603 | 2.48382 | 2.77719 |
| p=1 $\mu$=0 | 2.89736 | 3.01400 | 3.36392 |
| $\mu$=0.01 | 2.78328 | 2.89533 | 3.23147 |
| $\mu$=0.02 | 2.48925 | 2.58947 | 2.89009 |
| $\mu$=0.03 | 2.11659 | 2.20180 | 2.45742 |
| p=2 $\mu$=0 | 2.75545 | 2.86651 | 3.19968 |
| $\mu$=0.01 | 2.64696 | 2.75365 | 3.07370 |
| $\mu$=0.02 | 2.36733 | 2.46275 | 2.74899 |
| $\mu$=0.03 | 2.01292 | 2.09405 | 2.33744 |

Table 5 Critical buckling temperature (ΔT) of FG nanoshell based on various material gradient index, nonlocal and strain gradient parameters (V=0, Ω=0, L=20R, R=100h).

| | $\lambda$=0 | $\lambda$=0.01 | $\lambda$=0.02 |
|---|---|---|---|
| p=0 $\mu$=0 | 135.776 | 141.341 | 158.036 |
| $\mu$=0.01 | 130.430 | 135.776 | 151.813 |
| $\mu$=0.02 | 116.651 | 121.432 | 135.775 |
| $\mu$=0.03 | 99.1872 | 103.253 | 115.449 |
| p=1 $\mu$=0 | 64.7395 | 67.3618 | 75.2285 |
| $\mu$=0.01 | 62.1905 | 64.7096 | 72.2665 |
| $\mu$=0.02 | 55.6206 | 57.8736 | 64.6322 |
| $\mu$=0.03 | 47.2937 | 49.2093 | 54.9561 |
| p=2 $\mu$=0 | 54.9647 | 57.1944 | 63.8834 |
| $\mu$=0.01 | 52.8006 | 54.9425 | 61.3681 |
| $\mu$=0.02 | 47.2227 | 49.1383 | 54.8851 |
| $\mu$=0.03 | 40.1530 | 41.7818 | 46.6683 |

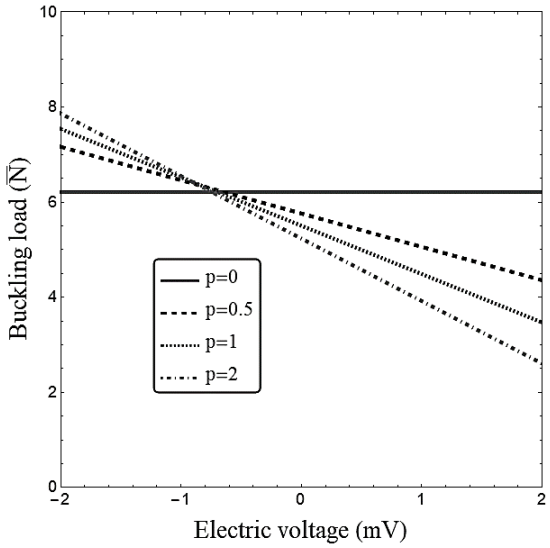


(a) CET: μ=0, λ=0

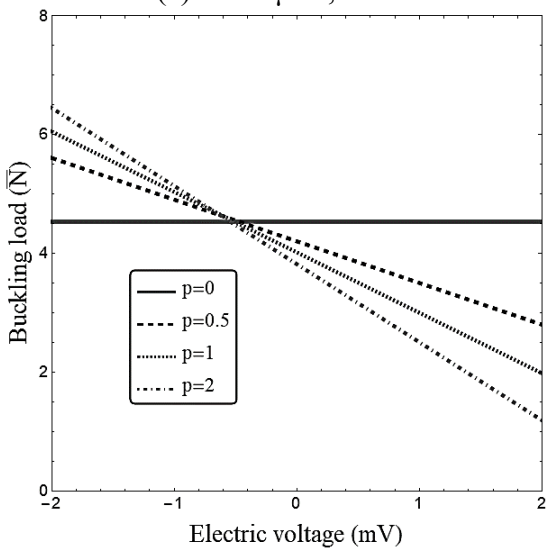


(b) NET: μ=0.03, λ=0

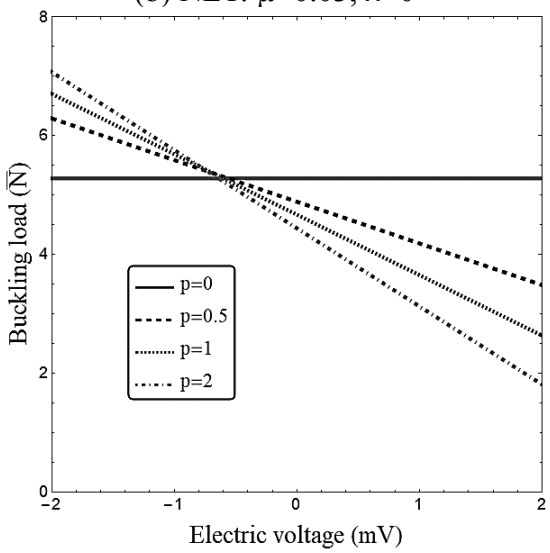


(c) NSGT: μ=0.03, λ=0.02

Fig. 2 Variation of critical buckling load with respect to electric voltage for different material exponents (R/h=100, L=20R, Ω=0).

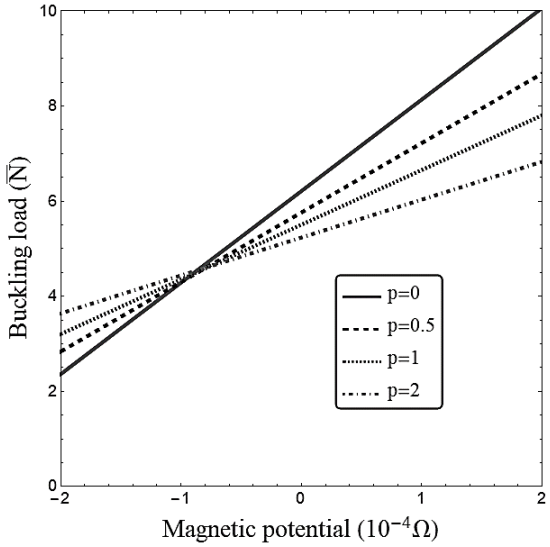


(a) CET: μ=0, λ=0

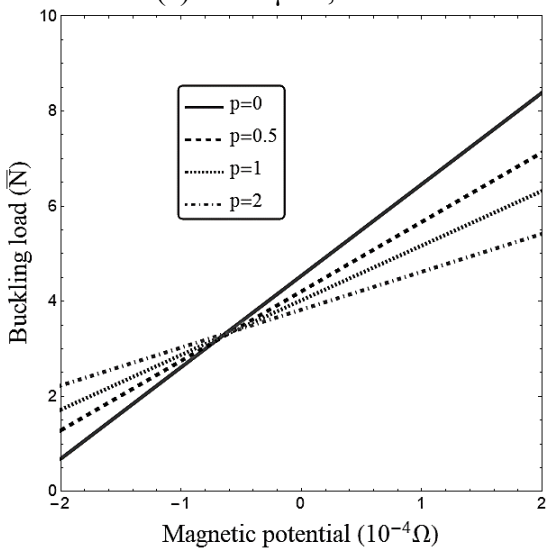


(b) NET: μ=0.03, λ=0

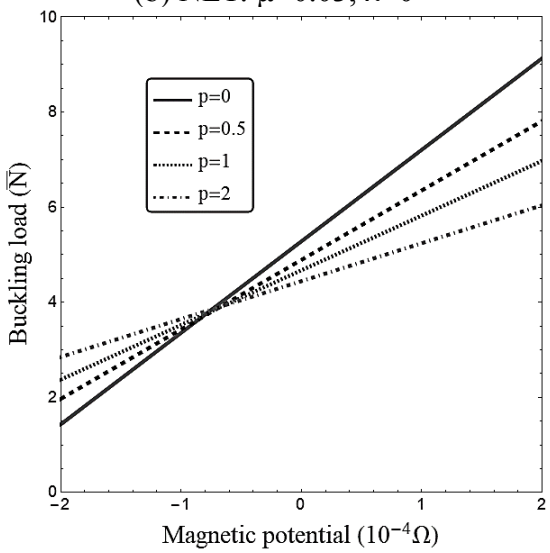


(c) NSGT: μ=0.03, λ=0.02

Fig. 3 Variation of critical buckling load with respect to magnetic potential for different material exponents (R/h=100, L=20R, V=0).

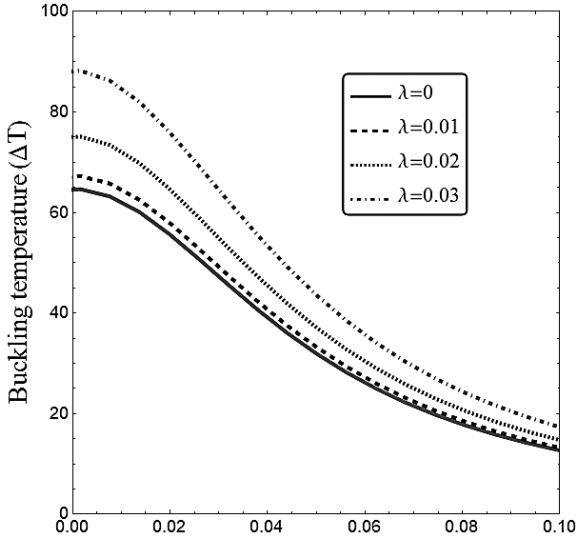


(a) UTR, S-S

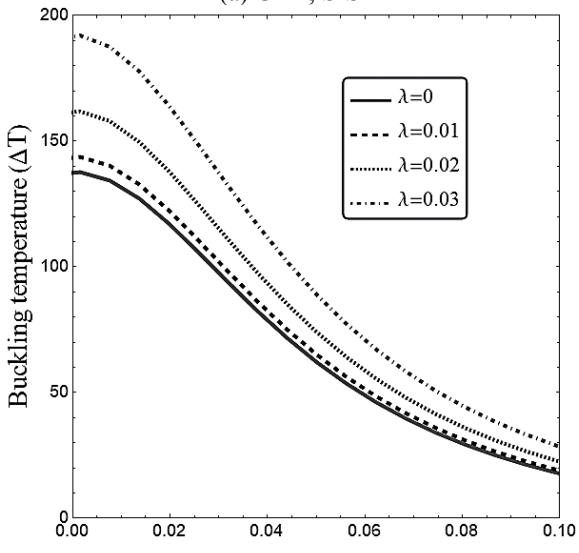


(b) LTR, S-S

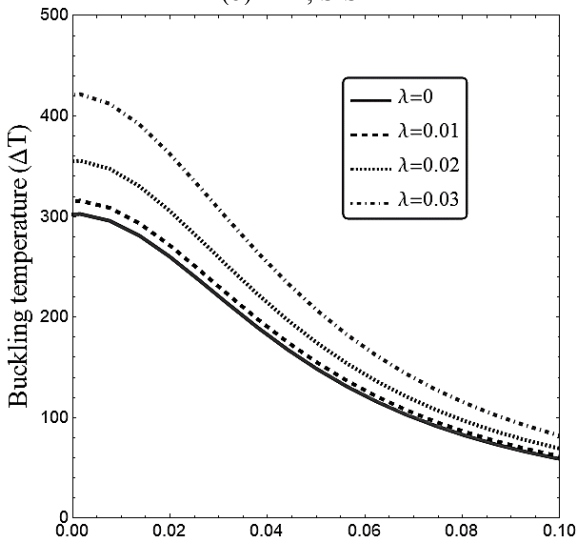


(c) UTR, C-C

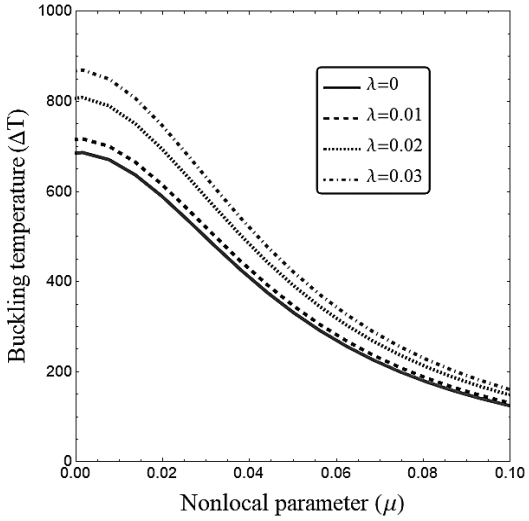


(d) LTR, C-C

Fig. 4 Buckling temperatures with respect to nonlocal parameter for different strain gradient parameters and temperature distributions (R/h=100, L=20R, p=1)

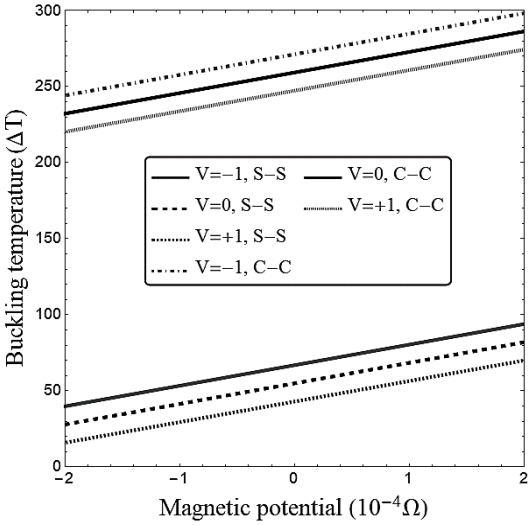


(a) UTR

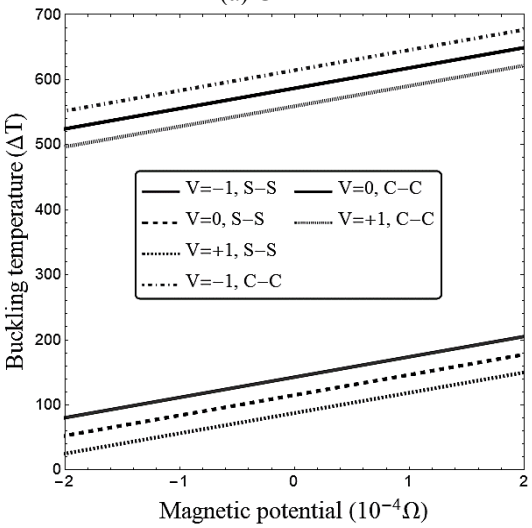


(b) LTR

Fig. 5 Critical buckling temperature of the nanoshell versus magnetic potential and various voltages (p=1, μ=0.03, λ=0.02).

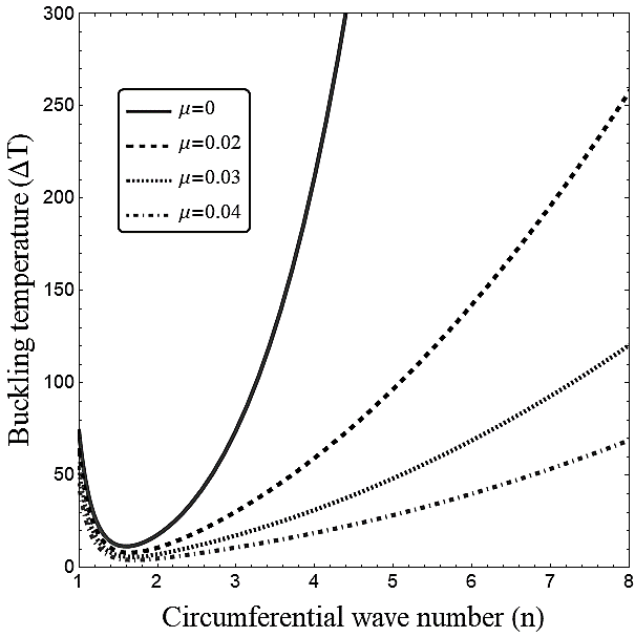


Fig. 6 Critical buckling temperature of the nanoshell versus wave number and various nonlocal parameter (R/h=50, L/R=20, V=0, Ω=0, p=1, λ=0.02)

## 6. Conclusions

In this paper, buckling characteristics of FG-METE nanoshells were studied in the framework of NSGT and classical shell theory. Different loadings such as electrical, mechanical, thermal and magnetic were exerted to the nanoshell. Temperature field had uniform and linear variation in nanoshell thickness. Five governing equations were developed for presented shell model and then they were solved using Galerkin's method. In was deduced that NSGT gives greater buckling loads than NET. This is because NSGT considers the influence of strain gradients and structural stiffness increment. However, NET only introduced structural stiffness reduction and gave smaller buckling loads than CET. Also, as the value of material exponent raised, the total portion of $CoFe_2O_4$ in FG material reduced and then the buckling load became more influenced by the electric voltage. Another observation was that UTR leads to lower critical temperatures than LTR. So, the nanoshell can tolerate higher temperatures in the case of LTR.

## References

Abualnour, M., Chikh, A., Hebali, H., Kaci, A., Tounsi, A., Bousahla, A. A. and Tounsi, A. (2019), "Thermomechanical analysis of antisymmetric laminated reinforced composite plates using a new four variable trigonometric refined plate theory", *Comput. Concrete*, **24**(6), 489-498. https://doi.org/10.12989/cac.2019.24.6.489.

Bedia, W. A., Houari, M. S. A., Bessaim, A., Bousahla, A. A., Tounsi, A., Saeed, T. and Alhodaly, M. S. (2019), "A New Hyperbolic Two-Unknown Beam Model for Bending and Buckling Analysis of a Nonlocal Strain Gradient Nanobeams", *J. Nano Res.*, **57**, 175-191.

https://doi.org/10.4028/www.scientific.net/JNanoR.57.175.

Addou, F. Y., Meradjah, M., Bousahla, A. A., Benachour, A., Bourada, F., Tounsi, A. and Mahmoud, S. R. (2019), "Influences of porosity on dynamic response of FG plates resting on Winkler/Pasternak/Kerr foundation using quasi 3D HSDT", *Comput. Concrete*, **24**(4), 347-367. https://doi.org/10.12989/cac.2019.24.4.347.

Ahmed, R.A., Fenjan, R.M., Luay Badr Hamad and Faleh, N. M. (2020), "A review of effects of partial dynamic loading on dynamic response of nonlocal functionally graded material beams", *Adv. Mater. Res.*, **9**(1), 33-48. https://doi.org/10.12989/amr.2020.9.1.033

Alasadi, A. A., Ahmed, R. A. and Faleh, N. M. (2019), "Analyzing nonlinear vibrations of metal foam nanobeams with symmetric and non-symmetric porosities", *Adv. Aircraft Spacecraft Sci.*, **6**(4), 273-282. https://doi.org/10.12989/aas.2019.6.4.273.

Alimirzaei, S., Mohammadimehr, M. and Tounsi, A. (2019), "Nonlinear analysis of viscoelastic micro-composite beam with geometrical imperfection using FEM: MSGT electro-magneto-elastic bending, buckling and vibration solutions", *Struct. Eng. Mech.*, **71**(5), 485-502. https://doi.org/10.12989/sem.2019.71.5.485.

Al-Maliki, A. F., Faleh, N. M. and Alasadi, A. A. (2019), "Finite element formulation and vibration of nonlocal refined metal foam beams with symmetric and non-symmetric porosities", *Struct. Monitor. Maintenance*, **6**(2), 147-159. https://doi.org/10.12989/smm.2019.6.2.147.

Arefi, M., Kiani, M. and Rabczuk, T. (2019), "Application of nonlocal strain gradient theory to size dependent bending analysis of a sandwich porous nanoplate integrated with piezomagnetic face-sheets", *Compos. Part B. Eng.*, **168**, 320-333. https://doi.org/10.1016/j.compositesb.2019.02.057.

Attia, M. A. and Mahmoud, F. F. (2016), "Modeling and analysis of nanobeams based on nonlocal-couple stress elasticity and surface energy theories", *J. Mech. Sci.*, **105**, 126-134. https://doi.org/10.1016/j.ijmecsci.2015.11.002.

AitYahia (2015), "Wave propagation in functionally graded plates with porosities using various higher-order shear deformation plate theories", *Struct. Eng. Mech.*, **53**(6), 1143 – 1165. doi.org/10.12989/sem.2015.53.6.1143.

Aissani, K., Bouiadjra, M. B., Ahouel, M. and Tounsi, A. (2015), "A new nonlocal hyperbolic shear deformation theory for nanobeams embedded in an elastic medium", *Struct. Eng. Mech.*, **55**(4), 743-763. https://doi.10.12989/sem.2015.55.4.743 .

Akgoz, B. and Civalek, O. (2013), "Buckling analysis of linearly tapered micro-columns based on strain gradient elasticity", *Struct. Eng. Mech.*, **48**(2), 195-205. doi.10.12989/sem.2013.48.2.195.

Barati, M. R. and Zenkour, A. M. (2018), "Electro-thermoelastic vibration of plates made of porous functionally graded piezoelectric materials under various boundary conditions", *J. Vib. Control*, **24**(10), 1910-1926. https://doi.org/10.1177%2F1077546316672788.

Barretta, R., Feo, L., Luciano, R., de Sciarra, F. M. and Penna, R. (2016), "Functionally graded Timoshenko nanobeams: a novel nonlocal gradient formulation", *Compos. Part B. Eng.*, **100**, 208-219. https://doi.org/10.1016/j.compositesb.2016.05.052.

Batou, B., Nebab, M., Bennai, R., Atmane, H. A., Tounsi, A. and Bouremana, M. (2019), "Wave dispersion properties in imperfect sigmoid plates using various HSDTs", *Steel Compos. Struct.*, **33**(5), 699. https://doi.org/10.12989/scs.2019.33.5.699.

Belbachir, N., Draich, K., Bousahla, A. A., Bourada, M., Tounsi, A. and Mohammadimehr, M. (2019), "Bending analysis of anti-symmetric cross-ply laminated plates under nonlinear thermal and mechanical loadings", *Steel Compos. Struct.*, **33**(1), 913-924. https://doi.org/10.12989/scs.2019.33.1.081.

Berghouti, H., Adda Bedia, E. A., Benkhedda, A. and Tounsi, A. (2019), "Vibration analysis of nonlocal porous nanobeams made of functionally graded material", *Adv. Nano Res.*, **7**(5), 351-364. https://doi.org/10.12989/anr.2019.7.5.351.

Berrabah, H. M., Tounsi, A., Semmah, A. and Adda, B. (2013), "Comparison of various refined nonlocal beam theories for bending, vibration and buckling analysis of nanobeams", *Struct. Eng. Mech.*, **48**(3), 351-365. https://doi.org/10.12989/sem.2013.48.3.351.

Bich, D. H., Nguyen, N. X. and Van Tung, H. (2013), "Postbuckling of functionally graded cylindrical shells based on improved Donnell equations", *Vietnam J. Mech.*, **35**(1), 1-15. https://doi.org/10.15625/0866-7136/35/1/2894.

Bousahla, A. A., Benyoucef, S., Tounsi, A. and Mahmoud, S. R. (2016), "On thermal stability of plates with functionally graded coefficient of thermal expansion", *Struct. Eng. Mech.*, **60**(2), 313-335. https://doi.org/10.12989/sem.2016.60.2.313.

Boukhlif, Z., Bouremana, M., Bourada, F., Bousahla, A. A., Bourada, M., Tounsi, A. and Al-Osta, M. A. (2019), "A simple quasi-3D HSDT for the dynamics analysis of FG thick plate on elastic foundation", *Steel Compos. Struct.*, **31**(5), 503-516. https://doi.org/10.12989/scs.2019.31.5.503.

Bourada, F., Bousahla, A. A., Bourada, M., Azzaz, A., Zinata, A. and Tounsi, A. (2019), "Dynamic investigation of porous functionally graded beam using a sinusoidal shear deformation theory", *Wind Struct.*, **28**(1), 19-30. https://doi.org/10.12989/was.2019.28.1.019.

Boutaleb, S., Benrahou, K. H., Bakora, A., Algarni, A., Bousahla, A. A., Tounsi, A., Tounsi, A. and Mahmoud, S. R. (2019), "Dynamic Analysis of nanosize FG rectangular plates based on simple nonlocal quasi 3D HSDT", *Adv. Nano Res.*, **7**(3), 189-206. http://dx.doi.org/10.12989/anr.2019.7.3.191.

Boulefrakh, L., Hebali, H., Chikh, A., Bousahla, A. A., Tounsi, A. and Mahmoud, S. R. (2019), "The effect of parameters of visco-Pasternak foundation on the bending and vibration properties of a thick FG plate", *Geomech. Eng.*, **18**(2), 161-178. https://doi.org/10.12989/gae.2019.18.2.161.

Chaabane, L. A., Bourada, F., Sekkal, M., Zerouati, S., Zaoui, F. Z., Tounsi, A., Derras, A., Bousahla, A. and Tounsi, A. (2019), "Analytical study of bending and free vibration responses of functionally graded beams resting on elastic foundation", *Struct. Eng. Mech.*, **71**(2), 185-196. https://doi.org/10.12989/sem.2019.71.2.185.

Chikh, A., Bakora, A., Heireche, H., Houari, M.S.A., Tounsi, A. and Bedia, E.A. (2016), "Thermo-mechanical postbuckling of symmetric S-FGM plates resting on Pasternak elastic foundations using hyperbolic shear deformation theory", *Struct. Eng. Mech.*, **57**(4), 617-639. https://doi.org/10.12989/sem.2016.57.4.617.

Draiche, K., Bousahla, A. A., Tounsi, A., Alwabli, A. S., Tounsi, A. and Mahmoud, S. R. (2019), "Static analysis of laminated reinforced composite plates using a simple first-order shear deformation theory. *Comput. Concrete*, **24**(4), 369-378. https://doi.org/10.12989/cac.2019.24.4.369.

Draoui, A., Zidour, M., Tounsi, A. and Adim, B. (2019), "Static and dynamic behavior of nanotubes-reinforced sandwich plates using (FSDT)", *J. Nano Res.*, **57**, 117-135. https://doi.org/10.4028/www.scientific.net/JNanoR.57.117.

Ebrahimi, F. and Barati, M. R. (2016), "Static stability analysis of smart magneto-electro-elastic heterogeneous nanoplates embedded in an elastic medium based on a four-variable refined plate theory", *Smart Mater. Struct.*, **25**(10), 105014. https://doi.org/10.1088/0964-1726/25/10/105014.

Ebrahimi, F. and Barati, M. R. (2018), "Vibration analysis of smart piezoelectrically actuated nanobeams subjected to magneto-electrical field in thermal environment", *J. Vib. Control.*, **24**(3), 549-564. https://doi.org/10.1177/1077546316646239.

Ebrahimi, F., Barati, M. R. and Dabbagh, A. (2016), "A nonlocal

strain gradient theory for wave propagation analysis in temperature-dependent inhomogeneous nanoplates", *J. Eng. Sci.*, **107**, 169-182. https://doi.org/10.1016/j.ijengsci.2016.07.008.

Ebrahimi, F. and Dabbagh, A. (2017), "On flexural wave propagation responses of smart FG magneto-electro-elastic nanoplates via nonlocal strain gradient theory", *Compos. Struct.*, **162**, 281-293. https://doi.org/10.1016/j.compstruct.2016.11.058.

Eltaher, M. A., Khater, M. E. and Emam, S. A. (2016), "A review on nonlocal elastic models for bending, buckling, vibrations, and wave propagation of nanoscale beams", *Appl. Math. Modell.*, **40**(5-6), 4109-4128. https://doi.org/10.1016/j.apm.2015.11.026.

Eringen, A. C. (1983), "On differential equations of nonlocal elasticity and solutions of screw dislocation and surface waves", *J. Appl. Physics*, **54**(9), 4703-4710. https://doi.org/10.1063/1.332803.

Ebrahimi, F. and Barati, M.R. (2018), "Wave propagation analysis of smart strain gradient piezo-magneto-elastic nonlocal beams", *Struct. Eng. Mech.,* **66**(2)*, 237-248*.https://doi.org/org/10.12989/sem.2018.66.2.237.

Ebrahimi, F., Shaghaghi, G. R. and Boreiry, M. (2016), "An investigation into the influence of thermal loading and surface effects on mechanical characteristics of nanotubes", *Struct. Eng. Mech.,* **57**(1), 179-200. https://doi.org/10.12989/sem.2016.57.1.179

Faleh, N. M., Fenjan, R. M. and Ahmed, R. A. (2020), "Forced vibrations of multi-phase crystalline porous shells based on strain gradient elasticity and pulse load effects", *J. Vib. Eng. Technol.*, 1-9. https://doi.org/10.1007/s42417-020-00203-8.

Farajpour, A., Yazdi, M. H., Rastgoo, A., Loghmani, M. and Mohammadi, M. (2016), "Nonlocal nonlinear plate model for large amplitude vibration of magneto-electro-elastic nanoplates", *Compos. Struct.*, **140**, 323-336. https://doi.org/10.1016/j.compstruct.2015.12.039.

Fenjan, R. M., Ahmed, R. A., Alasadi, A. A. and Faleh, N. M. (2019a), "Nonlocal strain gradient thermal vibration analysis of double-coupled metal foam plate system with uniform and non-uniform porosities", *Coupled Syst. Mech.*, **8**(3), 247-257. https://doi.org/10.12989/csm.2019.8.3.247.

Fenjan, R. M., Ahmed, R. A. and Faleh, N. M. (2019b), "Investigating dynamic stability of metal foam nanoplates under periodic in-plane loads via a three-unknown plate theory", *Adv. Aircraft Spacecraft Sci.*, **6**(4), 297-314. https://doi.org/10.12989/aas.2019.6.4.297.

Fenjan, R. M., Hamad, L. B. and Faleh, N. M. (2020), "Mechanical-hygro-thermal vibrations of functionally graded porous plates with nonlocal and strain gradient effects", *Adv. Aircraft Spacecraft Sci.*, **7**(2), 169-186. https://doi.org/10.12989/aas.2020.7.2.169.

Heydarpour, Y. and Malekzadeh, P. (2019), "Dynamic stability of cylindrical nanoshells under combined static and periodic axial loads", *J. Brazilian Soc. Mech. Sci. Eng.*, **41**(4), 184. https://doi.org/10.1007/s40430-019-1675-1.

Hanifi Hachemi Amar, L., Kaci, A. and Tounsi, A. (2017), "On the size-dependent behavior of functionally graded micro-beams with porosities", *Struct. Eng. Mech.*, **64**(5), 527-541. https://doi.org/10.12989/sem.2017.64.5.527 .

Hadji, L., HassaineDaouadji, T., Ait Amar Meziane, M. and Tlidji, Y., (2016), "Analysis of functionally graded beam using a new first-order shear deformation theory", *Struct. Eng. Mech.*, **57**(2), 315-325. https://doi.org/10.12989/sem.2016.57.2.315 .

Hamad, L. B., Khalaf, B. S. and Faleh, N. M. (2019), "Analysis of static and dynamic characteristics of strain gradient shell structures made of porous nano-crystalline materials", *Adv. Mater. Res.*, **8**(3), 179. https://doi.org/10.12989/amr.2019.8.3.179.

Hellal, H., Bourada, M., Hebali, H., Bourada, F., Tounsi, A., Bousahla, A. A. and Mahmoud, S. R. (2019), "Dynamic and stability analysis of functionally graded material sandwich plates in hygro-thermal environment using a simple higher shear deformation theory", *J. Sandwich Struct. Mater.*, (Accepted), https://doi.org/10.1177/1099636219845841.

Hussain, M., Naeem, M. N., Tounsi, A. and Taj, M. (2019), "Nonlocal effect on the vibration of armchair and zigzag SWCNTs with bending rigidity", *Adv. Nano Res.*, **7**(6), 431-442. https://doi.org/10.12989/anr.2019.7.6.431.

Karami, B., Janghorban, M. and Tounsi, A. (2019a), "Wave propagation of functionally graded anisotropic nanoplates resting on Winkler-Pasternak foundation", *Struct. Eng. Mech.*, **7**(1), 55-66. https://doi.org/10.12989/sem.2019.70.1.055.

Karami, B., Janghorban, M. and Tounsi, A. (2019b), "On exact wave propagation analysis of triclinic material using three dimensional bi-Helmholtz gradient plate model", *Struct. Eng. Mech.*, **69**(5), 487-497. https://doi.org/10.12989/sem.2019.69.5.487.

Karami, B., Janghorban, M. and Tounsi, A. (2019c), "On pre stressed functionally graded anisotropic nanoshell in magnetic field", *J. Brazilian Soc. Mech. Sci. Eng.*, **41**, 495. https://doi.org/10.1007/s40430-019-1996-0.

Karami, B., Janghorban, M. and Tounsi, A. (2020), "Novel study on functionally graded anisotropic doubly curved nanoshells", *Eur. Phys. J. Plus* 135, 103. https://doi.org/10.1140/epjp/s13360-019-00079-y.

Kaddari, M., Kaci, A., Bousahla, A. A., Tounsi, A., Bourada, F., Tounsi, A., Bedia, E.A. and Al-Osta, M. A. (2020), "A study on the structural behavior of functionally graded porous plates on elastic foundation using a new quasi-3D model: Bending and Free vibration analysis", *Comput. Concrete*, **25**(1), 37-57. https://doi.org/10.12989/cac.2020.25.1.037.

Khiloun, M., Bousahla, A. A., Kaci, A., Bessaim, A., Tounsi, A. and Mahmoud, S. R. (2019), "Analytical modeling of bending and vibration of thick advanced composite plates using a four-variable quasi 3D HSDT", *Eng. Comput.*, https://doi.org/10.1007/s00366-019-00732-1.

Kocaturk, T. and Akbas, S. D. (2013), "Wave propagation in a microbeam based on the modified couple stress theory", *Struct. Eng. Mech.,* **46**(3), 417-431. https://doi.org/10.12989/sem.2013.46.3.417.

Ke, L. L. and Wang, Y. S. (2014), "Free vibration of size-dependent magneto-electro-elastic nanobeams based on the nonlocal theory", *Physica E Low-dimensional Syst. Nanostruct.*, **63**, 52-61. https://doi.org/10.1016/j.physe.2014.05.002.

Ke, L. L., Wang, Y. S., Yang, J. and Kitipornchai, S. (2014), "The size-dependent vibration of embedded magneto-electro-elastic cylindrical nanoshells", *Smart Mater. Struct.*, **23**(12), 125036. https://doi.org/10.1088/0964-1726/23/12/125036.

Khalaf, B. S., Fenjan, R. M. and Faleh, N. M. (2019), "Analyzing nonlinear mechanical-thermal buckling of imperfect micro-scale beam made of graded graphene reinforced composites", *Adv. Mater. Res.*, **8**(3), 219. https://doi.org/10.12989/amr.2019.8.3.219.

Kunbar, L. A. H., Alkadhimi, B. M., Radhi, H. S. and Faleh, N. M. (2020), "Flexoelectric effects on dynamic response characteristics of nonlocal piezoelectric material beam", *Adv. Mater. Res.*, **8**(4), 259. https://doi.org/10.12989/amr.2019.8.4.259.

Li, L. and Hu, Y. (2015), "Buckling analysis of size-dependent nonlinear beams based on a nonlocal strain gradient theory", *J. Eng. Sci.*, **97**, 84-94. https://doi.org/10.1016/j.ijengsci.2015.08.013.

Li, L. and Hu, Y. (2016), "Nonlinear bending and free vibration analyses of nonlocal strain gradient beams made of functionally graded material", *J. Eng. Sci.*, **107**, 77-97. https://doi.org/10.1016/j.ijengsci.2016.07.011.

Lu, L., Guo, X. and Zhao, J. (2017), "Size-dependent vibration

analysis of nanobeams based on the nonlocal strain gradient theory", *J. Eng. Sci.*, **116**, 12-24. https://doi.org/10.1016/j.ijengsci.2017.03.006.

Ma, L. H., Ke, L. L., Reddy, J. N., Yang, J., Kitipornchai, S. and Wang, Y. S. (2018), "Wave propagation characteristics in magneto-electro-elastic nanoshells using nonlocal strain gradient theory", *Compos. Struct.*, **199**, 10-23. https://doi.org/10.1016/j.compstruct.2018.05.061.

Mahmoudi, A., Benyoucef, S., Tounsi, A., Benachour, A., Adda Bedia, E. A. and Mahmoud, S. R. (2019), "A refined quasi-3D shear deformation theory for thermo-mechanical behavior of functionally graded sandwich plates on elastic foundations", *J. Sandwich Struct. Mater.*, **21**(6), 1906-1926. https://doi.org/10.1177%2F1099636217727577.

Medani, M., Benahmed, A., Zidour, M., Heireche, H., Tounsi, A., Bousahla, A. A. (2019), "Static and dynamic behavior of (FG-CNT) reinforced porous sandwich plate", *Steel Compos. Struct.*, **32**(5), 595-610. https://doi.org/10.12989/scs.2019.32.5.595.

Meksi, R., Benyoucef, S., Mahmoudi, A., Tounsi, A., Adda Bedia, E. A. and Mahmoud, S. R. (2019), "An analytical solution for bending, buckling and vibration responses of FGM sandwich plates", *J. Sandw. Struct. Mater.*, **21**(2), 727-757. https://doi.org/10.1177/1099636217698443.

Mehralian, F., Beni, Y. T. and Zeverdejani, M. K. (2017a), "Calibration of nonlocal strain gradient shell model for buckling analysis of nanotubes using molecular dynamics simulations", *Physica B Condensed Matter*, **521**, 102-111. https://doi.org/10.1016/j.physb.2017.06.058.

Mehralian, F., Beni, Y. T. and Zeverdejani, M. K. (2017b), "Nonlocal strain gradient theory calibration using molecular dynamics simulation based on small scale vibration of nanotubes", *Physica B Condensed Matter*, **514**, 61-69. https://doi.org/10.1016/j.physb.2017.03.030.

Pan, E. (2001), "Exact solution for simply supported and multilayered magneto-electro-elastic plates", *J. Appl. Mech.*, **68**(4), 608-618. https://doi.org/10.1115/1.1380385.

Park, W. T., Han, S. C., Jung, W. Y and Lee, W. H. (2016), "Dynamic instability analysis for S-FGM plates embedded in Pasternak elastic medium using the modified couple stress theory", *Steel Compos. Struct.*, **22**(6), 1239-1259. https://doi.org/10.12989/scs.2016.22.6.1239.

Pour, H. R., Vossough, H., Heydari, M. M., Beygipoor, G. and Azimzadeh, A. (2015), "Nonlinear vibration analysis of a nonlocal sinusoidal shear deformation carbon nanotube using differential quadrature method", *Struct. Eng. Mech.*, **54**(6), 1061-1073. https://doi.org/10.12989/sem.2015.54.6.1061.

Ramirez, F., Heyliger, P. R. and Pan, E. (2006), "Free vibration response of two-dimensional magneto-electro-elastic laminated plates", *J. Sound Vib.*, **292**(3-5), 626-644. https://doi.org/10.1016/j.jsv.2005.08.004.

Sayyad, A. S. and Ghugal, Y. M. (2018), "An inverse hyperbolic theory for FG beams resting on Winkler-Pasternak elastic foundation", *Adv. Aircraft Spacecraft Sci.*, **5**(6), 671-689. https://doi.org/10.12989/aas.2018.5.6.671.

Sahla, M., Saidi, H., Draiche, K., Bousahla, A. A., Bourada, F. and Tounsi, A. (2019), "Free vibration analysis of angle-ply laminated composite and soft core sandwich plates", *Steel Compos. Struct.*, **33**(5), 663-679. https://doi.org/10.12989/scs.2019.33.5.663.

Semmah, A., Heireche, H., Bousahla, A.A., Tounsi, A. (2019), "Thermal buckling analysis of SWBNNT on Winkler foundation by nonlocal FSDT", *Adv. Nano Res.*, **7**(2), 89-98. http://dx.doi.org/10.12989/anr.2019.7.2.089.

She, G. L., Yuan, F. G., Ren, Y. R., Liu, H. B. and Xiao, W. S. (2018), "Nonlinear bending and vibration analysis of functionally graded porous tubes via a nonlocal strain gradient theory", *Compos. Struct.*, **203**, 614-623. https://doi.org/10.1016/j.compstruct.2018.07.063.

Şimşek, M. (2019), "Some closed-form solutions for static, buckling, free and forced vibration of functionally graded (FG) nanobeams using nonlocal strain gradient theory", *Compos. Struct.*, **224**, 111041. https://doi.org/10.1016/j.compstruct.2019.111041.

Taghizadeh, M., Ovesy, H. R. and Ghannadpour, S. A. M. (2015), "Nonlocal integral elasticity analysis of beam bending by using finite element method", *Struct. Eng. Mech.*, **54**(4), 755-769. https://doi.org/10.12989/sem.2015.54.4.755 .

Tlidji, Y., Zidour, M., Draiche, K., Safa, A., Bourada, M., Tounsi, A., Bousahla, A. and Mahmoud, S. R. (2019), "Vibration analysis of different material distributions of functionally graded microbeam", *Struct. Eng. Mech.*, **69**(6), 637-649. https://doi.org/10.12989/sem.2019.69.6.637.

Tounsi, A., Houari, M. S. A. and Bessaim, A. (2016), "A new 3-unknowns non-polynomial plate theory for buckling and vibration of functionally graded sandwich plate", *Struct. Eng. Mech.*, **60**(4), 547-565. https://doi.org/10.12989/sem.2016.60.4.547 .

Waksmanski, N. and Pan, E. (2017), "An analytical three-dimensional solution for free vibration of a magneto-electro-elastic plate considering the nonlocal effect", *J. Intelligent Mater. Syst. Struct.*, **28**(11), 1501-1513. https://doi.org/10.1177/1045389X16672734.

Yazid, M., Heireche, H., Tounsi, A., Bousahla, A.A. and Houari, M. S. A. (2018), "A novel nonlocal refined plate theory for stability response of orthotropic single-layer graphene sheet resting on elastic medium", *Smart Struct. Syst.,* **21**(1), 15-25. https://doi.org/10.12989/sem.2018.68.6.661.

Zarga, D., Tounsi, A., Bousahla, A. A., Bourada, F. and Mahmoud, S. R. (2019), "Thermomechanical bending study for functionally graded sandwich plates using a simple quasi-3D shear deformation theory", *Steel Compos. Struct.*, **32**(3), 389-410. https://doi.org/10.12989/scs.2019.32.3.389.

Zaoui, F. Z., Ouinas, D. and Tounsi, A. (2019), "New 2D and quasi-3D shear deformation theories for free vibration of functionally graded plates on elastic foundations", *Compos. Part B*, **159**, 231-247. https://doi.org/10.1016/j.compositesb.2018.09.051.

Zemri, A., Houari, M. S. A., Bousahla, A. A. and Tounsi, A. (2015), "A mechanical response of functionally graded nanoscale beam: an assessment of a refined nonlocal shear deformation theory beam theory", *Struct. Eng. Mech.*, **54**(4), 693-710. https://doi.org/10.12989/sem.2015.54.4.693

Zeighampour, H., Beni, Y. T. and Dehkordi, M. B. (2018), "Wave propagation in viscoelastic thin cylindrical nanoshell resting on a visco-Pasternak foundation based on nonlocal strain gradient theory", *Thin-Walled Struct.*, **122**, 378-386. https://doi.org/10.1016/j.tws.2017.10.037.

*CC*